Journal of Fluorescence, Vol. 6, No. 4, 1996

Spectroscopic and Photophysical Investigations on the Nature of Localization of Rhodamine-123 and Its Dibromo Derivative in Different Cell Lines

Luc Villeneuve,[1,4] Prabir Pal,[2] Gilles Durocher,[2,4] David Migneault,[3] Denis Girard,[3] Richard Giasson,[3,4] Antonia Balassy,[1] Louise Blanchard,[1] and Louis Gaboury[1,4]

Received May 1, 1996; accepted October 2, 1996

Steady-state and time-resolved spectroscopic properties of rhodamine-123 (**rh123**) and 4,5-dibromorhodamine methyl ester (**dbr123**) bound to different cell lines are evaluated. Studies are also performed on the dye bound to extracted mitochondria. Results are compared with those obtained in homogeneous and microheterogeneous media. Results suggest that these dyes can specifically bind only with cell mitochondria. As a result of binding, excitation and emission spectra are red shifted by 10 to 12 nm. The fluorescence decay of these dyes bound to mitochondria shows two lifetimes. Values are about 4.0 and 2.0 ns for **rh123** and about 1.9 and 0.5 ns for **dbr123**. Detailed global analysis of emission wavelength and dye concentration dependences of the fluorescence decay is performed. Results indicate that these dyes are bound to two different binding sites at mitochondria. The decay-associated fluorescence spectrum for the species corresponding to each binding site is recovered. Species **1**, corresponding to the longer lifetime, is found to be more red shifted compared to species **2**. The fluorescence of species **2** is heavily quenched. The origin of this quenching is explained in terms of resonance energy transfer between donor species **2** and acceptor species **1**. The possible nature of the two binding sites is also discussed.

KEY WORDS: Rhodamine-123; 4,5-dibromorhodamine methyl ester; localization; spectroscopic properties.

INTRODUCTION

Rhodamine-123 (*rh123*) has been extensively employed as a fluorescence stain of mitochondria in living cells.[1-3] The transmembrane potential at the inner membrane system has been reported to be responsible for the accumulation of this dye at mitochondria.[4,5] **Rh123** was also known to be non- or weakly phototoxic due to its inefficiency of singlet oxygen production.[6] Recently, we have synthesized one dibrominated cationic rhodamine dye, namely, 4,5-dibromorhodamine methyl ester (**dbr123**), which is also equally efficient to stain mitochondria, for the purpose of efficient cancer cell photosensitization. In a recent work, we have shown that **dbr123** is an efficient singlet oxygen producer and could be used as an efficient cancer cell photosensitiser for potential uses in *in vitro* bone marrow purging in preparation for autologous bone marrow transplantation.[7] The extent of photodynamic action depends not only on the singlet oxygen production but also on the biodistribution of the ionic dye in the cytoplasmic and mito-

[1] Laboratoire de phathologie moléculaire, Département de pathologie, Université de Montréal, C.P. 6128, Succ. Centre-ville, Montréal, Québec H3C 3J7, Canada.
[2] Laboratoire de photophysique moléculaire, Département de chimie, Université de Montréal, C.P. 6128, Succ. Centre-ville, Montréal, Québec H3C 3J7, Canada.
[3] Laboratoire de photochimie organique, Département de chimie, Université de Montréal, C.P. 6128, Succ. Centre-ville, Montréal, Québec H3C 3J7, Canada.

1053-0509/96/1200-0209$09.50/0

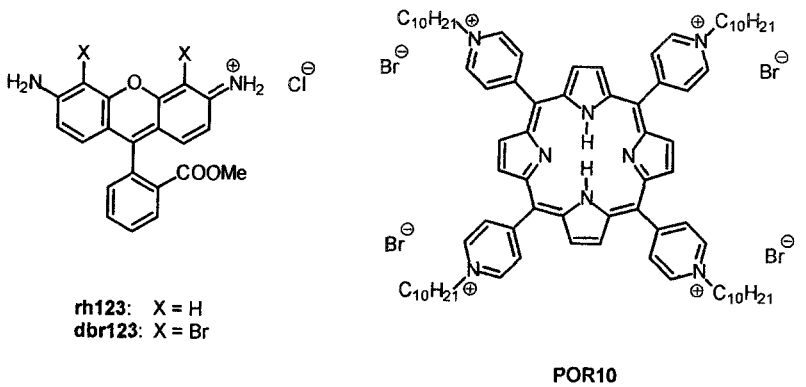

Fig. 1. Molecular structures of **rh123**, **dbr123**, and **POR10**.

chondrial membranes, the retention, and the nature of the binding inside the cell. The binding sites and the microenvironment surrounding dye molecules inside the cell are indeed complex in nature and influence the photophysical properties of the dye. Fluorescence microscopy has been used to study the cellular drug distribution. Even by using a confocal microscope, the accurate identification of cytoplasmic organelles and of drug binding sites remains uncertain.[8]

Among the various techniques employed to probe the nature of binding of drug inside the cell, fluorescence has turned out to be one of the most powerful techniques due to its excellent sensitivity and its time domain.[9,10] Especially, time-resolved spectroscopy is the ideal technique to unravel the often complex kinetics of excited-state processes. Global analysis[11] of fluorescence decay traces obtained under different experimental conditions are now considered a powerful tool to extract the physical significances of the decay data[12] in complex biological systems.

Micellar media are considered as simple membrane mimetic systems.[13] Over the past few decades, there has been widespread interest in studying spectroscopic and photophysical properties of photosensitizing dyes in micellar media, for a better understanding of the nature of localization and interaction in true biological systems. It is very important to know the spectroscopic and photophysical properties of the dye in micellar environments to interpret the results obtained in true cell systems.

We have recently reported spectroscopic and photophysical characterizations of **rh123** and **dbr123** in anionic sodium dodecylsulfate (SDS), cationic cetyltrimethylammonium bromide (CTAB), and neutral TX 100 (TX) micellar media.[14] In this paper, we report the steady-state and time-resolved fluorescence properties of **rh123** and **dbr123** in different cell lines and in their extracted mitochondria. The molecular environment of these dyes in the true biological system is discussed using environmentally sensitive spectroscopic and photophysical properties in different homogeneous and micellar media.

MATERIALS AND METHODS

Materials

Rhodamine-123 (Aldrich) was used as received after checking purity by HPLC. 4,5-Dibromorhodamine methyl ester (**dbr123**) was synthesized in our laboratory. Details of the synthesis and purification are described elsewhere.[7]. The purity of the synthesized dye is superior to 99%. The porphyrin derivative 5,10,15,20-Tetrakis (1-decylpyridinium-4-yl)-21H,23H-porphyrin tetrabromide (**POR10**) was synthesized and purified according to Okuno *et al.*.[15] Molecular structures of **rh123**, **dbr123**, and **POR10** are shown in Fig. 1. Spectrophotometric-grade solvents were used as received. The surfactants, SDS (Aldrich; 98%) and CTAB (Aldrich; 95%), were used after being purified according to the method reported recently.[16] TX (Fluka; 99%) was used as received. Doubly distilled deionized water was used as solvent. The pH of the water and of the micellar media was maintained at about 6.3. All these dyes are in esterified form and no pH effect was observed within the range of 1 to 12.[17]

Cell Preparation

The human erythroleukemic cell line, K562, rat fibroblastic cell line, RAT 2, and KG1 cell line were ob-

tained from the American Type Culture Collection (Rockville, MD). All the cells were grown according to the donor's specifications. Briefly, K562 were grown in Dulbecco minimal essential medium (DMEM) supplemented with 10% in activated fetal bovine serum (FBS) with 1% antibiotics (penicillin, 1000 U/ml; streptomycin, 1000 U/ml; and gentamycin, 10 μg/ml) and passaged three times a week. Adherent cells (RAT 2) were grown to 90–100% confluency and nonadherent cell lines (K562 and KG1) were grown in suspension to a concentration of 0.8 million cells per ml before each experiment. Cell viability was always over 95% in all experiments as evaluated by trypan blue exclusion. Cells were incubated at final concentrations of 5 to 20 $\times$ 10^6 cells per 100-mm petri dish for 30 min in DMEM with 10% serum and dye at the required concentration. Immediately after incubation, cells are washed two times with Dulbecco phosphate-buffered saline (DPBS) and transferred into a 1-mm-path length quartz cuvette. The cuvette is then centrifuged at 1000 *g* for 2 minutes, to deposit all the cells at the bottom of the cuvette. Spectroscopic measurements were performed immediately after cell preparation.

Preparation of Mitochondria

Mitochondria were isolated from 1–2 $\times$ 10^9 cells in a medium (isolation buffer) containing ice-cold 70 m*M* sucrose, 210 m*M* mannitol, 5 m*M* Tris, pH 7.5, 2.5 m*M* ETDA, 2.5 m*M* EGTA, 0.1 m*M* PMSF, 1 m*M* dithiothreitol, 1 μg/ml leupeptine, and 5 μg/ml aprotinin. The method of isolation is similar to that described elsewhere.[18] Briefly, cells were disrupted with 15 strokes of a motor-driven iced pestle and the homogenate centrifuged at 1000 *g* for 3 min. After discarding the pellet, the supernatant is centrifuged at 27,000 *g* for 20 min. The pellet is resuspended in isolation buffer, and layered on a discontinuous sucrose (1/1.5 *M*) gradient, and centrifuged at 80,000 *g* for 10 min at 4°C. Mitochondria are recovered from the interface, transferred to an Eppendorf tube, and washed twice in isolation buffer before use in the experiments.

Spectroscopic Studies

The absorption spectra were recorded on a Philips PU-8800 UV–visible spectrophotometer. Corrected fluorescence spectra were recorded on a Spex Fluorolog-2 spectrofluorometer with a F2T11 special configuration. Fluorescence lifetimes were measured on a multiplexed time-correlated single-photon counting fluorometer (Edinburgh Instruments, Model 299T). Details of the instrumental setup are described elsewhere.[19] For spectroscopic measurements in water, DPBS, and micellar medium, the dye concentration was always kept below 2 $\times$ 10^{-6} *M* in order to avoid dye aggregation and reabsorption effects. To avoid any aggregation, we checked that the Beer–Lambert law is valid in the concentration range we have studied. Freshly prepared solutions were always used. Spectroscopic measurements with cell lines and with mitochondria were done in front-face mode. The front face of the cuvette was placed at 22.5° to the excitation beam and emission was collected at a right angle to the excitation beam.

The analysis of the entire decay including the rising edge was performed by the deconvolution method. The goodness of fit has been assessed from the statistical parameters χ^2 and DW (Durbin–Watson).[19] Lifetime data were also analyzed by the global analysis method assuming that the fluorescence decay can be represented as a sum of exponential components:

$$I(t) = \sum_i \alpha_i \exp(-t/\tau_i) \quad (1)$$

where τ_i and α_i are the lifetime and the preexponential factor of the *i*th component, respectively. A global iterative reweighted reconvolution program based on a nonlinear least-squares method was used (Global Unlimited, Urbana, IL).[20] Lifetime data were both individually and globally analyzed by using, single, double, or triple exponentials and also by using some other different decay functions pertinent for the energy transfer mechanism. To obtain the influence of the dye concentration during incubation on the fluorescence lifetime and to recover decay-associated spectra (DAS) of the species corresponding to each lifetime, decays were measured at different dye concentrations during incubation and at different emission wavelengths, respectively, and were analyzed globally by linking the lifetime and allowing the α's to float independently. The preexponential factors were normalized and the fractional fluorescence intensity was calculated as

$$I_i = \alpha_i \tau_i / \sum_i \alpha_i \tau_i \quad (2)$$

The wavelength dependence of each fraction multiplied by steady-state fluorescence intensity at the corresponding wavelength produces the DAS of each corresponding species. The sum of these fractions at a particular wavelength should be proportional to the steady-state intensity measured at the corresponding wavelength.

Table I. Spectroscopic and Photophysical Data of rh123 and dbr123 in Water, Ethanol, DPBS, Different Micellar Media, Different Cell Lines, and Extracted Mitochondria

Dye	Medium	Abs./ex. max (nm)	Em. max (nm)	ϕ_F	τ_i (α_i) (ns)[a]
rh123	H_2O	498	525	0.87	4.2
	Ethanol	507	531	0.86	4.0
	DPBS	498	525	0.86	4.1
	SDS (0.05 *M*)	507	532	0.83	4.5
	CTAB (0.17 *M*)	498	525	0.91	3.9
	TX (0.017 *M*)	510	535	0.62	4.2 (0.30)
					3.2 (0.70)
	K562 cell	511	536		4.0 (0.69)
					2.0 (0.31)
	KG1 cell	512	536		4.1 (0.71)
					2.1 (0.29)
	Rat 2 cell	511	535		4.2 (0.67)
					2.2 (0.33)
	Mitochondria (K562)	512	535		3.9 (0.70)
					2.0 (0.30)
	Mitochondria (KG1)	513	537		4.1 (0.69)
					2.0 (0.31)
dbr123	H_2O	504	531	0.34	1.7
	Ethanol	513	538	0.52	2.5
	DPBS	505	532	0.33	1.7
	SDS (0.05 *M*)	512	538	0.35	2.1
	CTAB (0.17 *M*)	506	534	0.26	2.1
	TX (0.017 *M*)	515	542	0.14	1.6 (0.35)
					0.76 (0.65)
	K562 cell	517	543		1.9 (0.54)
					0.41 (0.46)
	KG1 cell	516	546		1.9 (0.68)
					0.50 (0.32)
	Rat 2 cell	517	544		1.9 (0.54)
					0.56 (0.46)
	Mitochondria (K562)	518	544		1.9 (0.67)
					0.57 (0.33)
	Mitochondria (KG1)	517	544		1.9 (0.66)
					0.54 (0.36)

[a]Fluorescence decays in cell lines, extracted mitochondria, and TX micelles are double exponential in nature. Values shown in parentheses are the corresponding normalized preexponential factors. In all other media decay is single exponential.

RESULTS AND DISCUSSION

Steady-State Spectroscopy

We have measured excitation and emission spectra for these dyes in different cell lines, *viz.*, metastatic K562 cell lines, KG1 cell lines, and normal Rat 2 cell lines. We have also measured the same in extracted mitochondria. Results are shown in Table I. Figure 2 shows the normalized excitation and emission spectra of **dbr123** in DPBS, in K562 cell lines, and in extracted

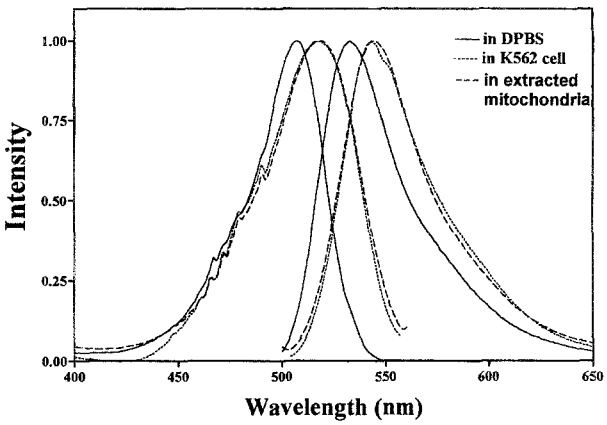

Fig. 2. Normalized excitation (λ_{em} = 560 nm) and emission ($\lambda_{exc.}$ = 480 nm) of **dbr123** in DPBS, K562 cell lines, and mitochondria extracted from K562 cells. For cell lines and mitochondria, the dye concentration during incubation is kept at 10 μ*M*.

mitochondria of K562 cell lines. It is observed that in the K562 cell line and also in the respective extracted mitochondria, both excitation and emission spectra are red shifted by 10–12 nm compared to that in DPBS. We are comparing the cell and mitochondria results with those in DPBS because the spectroscopic properties of these dyes in DPBS, the natural medium where the cells and mitochondria are suspended for our studies, can be considered as the properties of free dye. From Table I, one can see that spectroscopic and photophysical properties of these dyes in water and in DPBS are the same. Fluorescence and excitation spectra in extracted mitochondria are almost identical to those obtained in cell lines. Similar results are obtained in other cell lines also (see Table I). **Rh123** also shows similar changes. Red-shifting of the fluorescence spectra may sometime arise due to the self-absorption effect if dye concentrations are very high. It is very difficult to ascertain the local dye concentration inside the cell and in mitochondria. It is important to note that all the data presented in Table I concerning cell lines and mitochondria are at an incubation dye concentration of 10 μ*M*. The concentration of the dye inside the cell and in mitochondria may not be exactly the same as the external concentration. The total cellular dye concentration depends on mitochondrial synthesis, which peaks at the S phase of the cell cycle,[21] on the transmembrane mitochondrial potential and hydrophobic interactions of the dye with the lipophilic component of the inner membrane,[3] and on the active transport out of the cell by protein transporters.[23] But the facts that (1) the absorption and excitation spectra of the rhodamines in water, ethanol, DPBS, and the various micelles are identical and (2) the excitation spec-

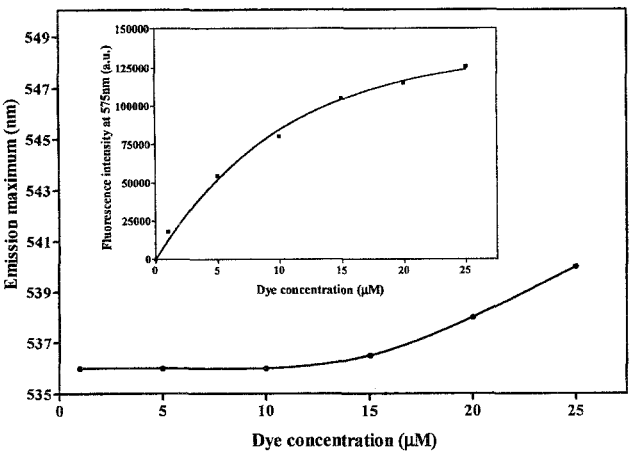

Fig. 3. Rh123 concentration during incubation vs. fluorescence maximum of **rh123** in K562 cell lines. Inset shows the variation of the fluorescence intensity (monitored at 575 nm, where the reabsorption effect should be negligible) of **rh123** in K562 cell lines with the **rh123** concentration during incubation.

tra in the cell lines and mitochondria are red-shifted by about the same amount as their fluorescence spectra compared to the spectra in DPBS are good indications that self-absorption is not playing role here.

To ascertain the importance of self-absorption, we have also studied the incubation dye concentration dependence on the fluorescence maximum. Figure 3 shows a representative plot of fluorescence maximum vs **rh123** concentration in the medium of incubation for K562 cell lines. Up to ~15 μM concentration, no shift in the emission maximum due to self-absorption is observed. At higher concentrations, self-absorption starts to play a role. But its contribution to the shift is small compared to the red shift we observed going from DPBS to K562 cells or mitochondria (≈11 nm). Therefore, we can safely assume that the red shift in fluorescence maxima reported in Table I are not due merely to the self-absorption effect. Extrapolation of the curve of the emission maximum vs dye concentration (Fig. 3) up to an 11-nm shift shows that a dye concentration as high as 45 μM inside the cell would be necessary for self-absorption to take place. This local concentration is considered much too high to obtain compared to the incubation dye concentration of 10 μM.[21,23] Moreover, the inset in Fig. 3 shows the variation of fluorescence intensity at longer wavelengths (where the reabsorption effect is negligible) with the dye concentration in the medium during incubation. One can see that the fluorescence intensity does not increase linearly with the external dye concentration. At higher dye concentrations, saturation behavior is observed.

From fluorescence microscopy, we have seen that these dyes are localized only in the mitochondrial region. This is true for both dyes. There is no fluorescence observed from other cellular compartments like the cytoplasm and cell nuclei. This observation together with the similar excitation and emission spectra of the dye in extracted mitochondria compared to those obtained in cell lines confirms that these two dyes bind only on the mitochondria. In fact, **rh123** is well-known for mitochondrial staining.[1,3] Our newly synthesized dye, **dbr123**, also behaves similarly.

In order to understand the physical significances of this red shift due to binding of the dye in the mitochondrial membrane, it is important to compare the results with the spectroscopic and photophysical properties of these dyes in the micellar media. Recently, we have reported the spectroscopic and photophysical properties of these dyes in anionic SDS, cationic CTAB, and neutral TX micelles.[14] Results are also retabulated in Table I. From this table, one can see that these dyes can bind only with SDS and TX micelles. There is hardly any interaction observed with CTAB micelles. Both in SDS and in TX micelles, absorption and emission spectra are red shifted compared to those in water. In TX micelles, shifts are more important. Our recent timeresolved fluorescence study[14] has revealed that the nature of interaction in SDS is quite different from that in TX. In SDS micelles, interaction is electrostatic in nature. Dyes are localized at the outer Stern layer of SDS micelles and the extent of the shift depends on the local polarity. In TX micelles, these dyes form strong ground-state complexes. As the electrostatic interaction is absent, complex formation is facilitated by hydrophobic interactions. The nature of the complex is rather of a charge-transfer type between the phenolic donor group (in TX) and the rhodamine acting as an electron acceptor.

If we compare the excitation and emission maxima obtained in cell lines and in extracted mitochondria to those obtained in SDS and in TX micellar media, we can see that the shifts are similar to those obtained in TX micelles. In fact, Millot *et al.*[23] compared the fluorescence of **rh123** bound to K562 cell lines and to multidrug-resistant K562-R cell lines to the fluorescence of **rh123** in TX micelles. But the matching of the excitation and fluorescence maxima does not necessarily imply that the binding is not electrostatic since it could also be due to a charge transfer-type complex formation with some proteins or enzymes. Actually, the mitochondria structure is very complex in nature. It is composed mainly of an inner and an outer lipid bilayer membrane. Several types of proteins and enzymes are also bound to these membranes (70% of contents). The inner and outer sides

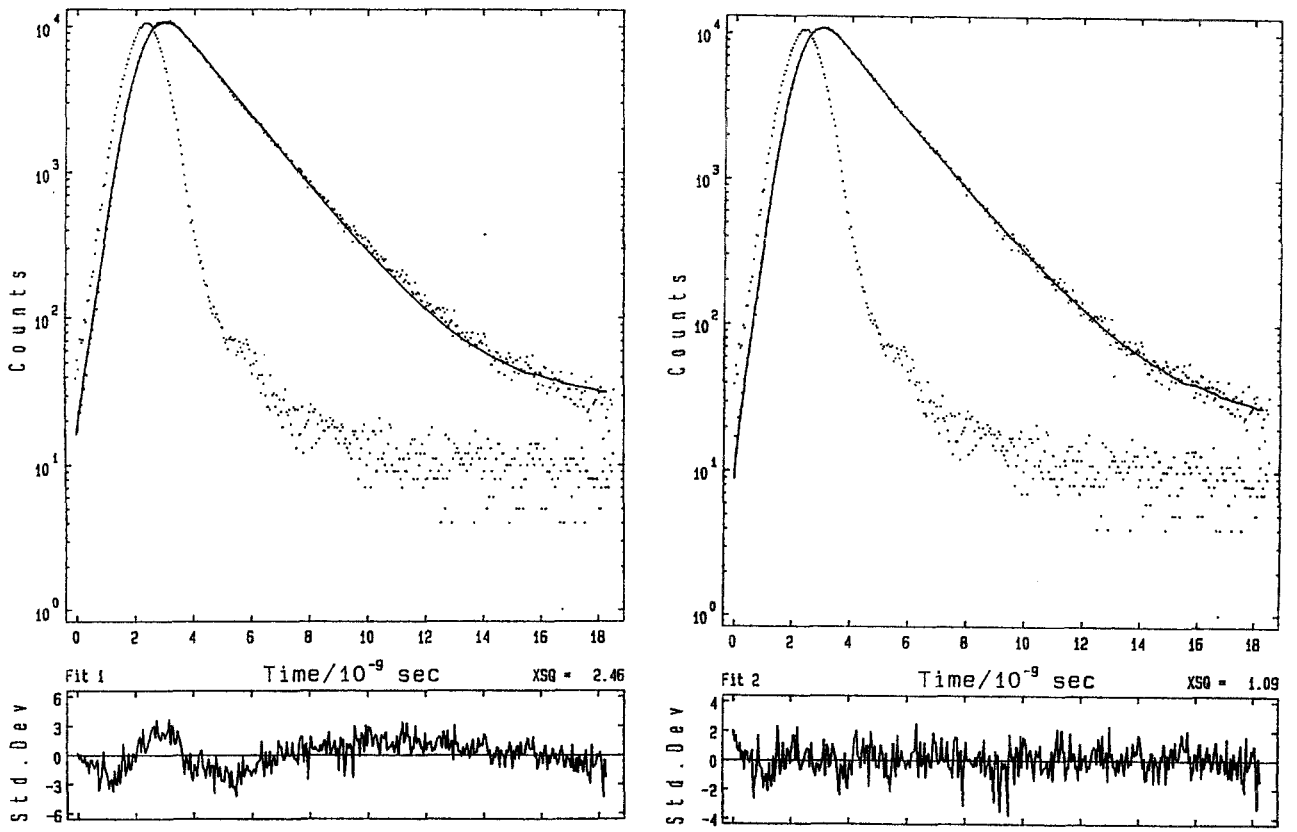

Fig. 4. Fluorescence decay curves associated with the lamp profiles for **dbr123** in isolated mitochondria of K562 cell lines. The curves from left to right show the single- and double-exponential fits, residual, and χ^2 for the same experimental data. Excitation and emission wavelengths are 480 and 540 nm, respectively.

of the mitochondrial membrane are negatively charged. Cationic dyes can be localized at the mitochondria due to the electrostatic interaction and/or can bind with proteins or enzymes. To shed some light on the specific nature and site of the dye binding, it appears important to study the fluorescence lifetime of the dye in cell lines and also in extracted mitochondria.

Time-Resolved Spectroscopy

We have measured the fluorescence decay of **rh123** and **dbr123** in normal and highly tumorigenic cell lines and also in extracted mitochondria. Unlike the homogeneous media and SDS micelles, where the fluorescence decay can best be described by a single-exponential fit, a double-exponential fit is necessary to analyze the decay data in cell lines and also in extracted mitochondria. This is true for both dyes. Figure 4 shows a representative fluorescence decay of **dbr123** in extracted mitochondria of K562 cell lines. The two lifetimes recovered and their respective normalized preexponential factors are tabulated in Table I. The longest components are about 3.9 and 1.9 ns for **rh123** and **dbr123**, respectively. The shortest components are about 2.0 and 0.5 ns for **rh123** and **dbr123**, respectively. Another interesting observation is that for a particular dye, the respective values of the two lifetimes as well as their respective preexponential factors, are almost independent of the nature of the cell lines (see Table I). No difference is observed between normal Rat2 fibroblasts and leukemic K562 or KG1 cell lines. This indicates that the nature of dye binding to the mitochondria is independent of whether the cell lines are metastatic or normal.

The observation of two lifetimes actually may indicate two different populations at two different sites of binding. Let us define the species corresponding to the longer lifetime as species **1** and that corresponding to the shorter one as species **2**. In order to get more information on the two species, we have studied the emission wavelength dependence on the fluorescence lifetimes. A series of decay data monitored at different emission wavelengths is analyzed globally by linking lifetimes

Table II. Fluorescence Wavelength-Dependent Global Analysis of the Fluorescence Decay of rh123 and dbr123 in K562 Cell Lines (Excitation Wavelength, 480 nm)

Dye	λ_{em} (nm)	τ_1 (ns)	α_1	I_1	τ_2 (ns)	α_2	I_2	Individual χ^2	Global χ^2
rh123	525	4.0	0.56	0.72	2.0	0.44	0.28	0.96	1.01
	530		0.63	0.77		0.37	0.23	1.01	
	535		0.70	0.82		0.30	0.18	0.96	
	540		0.74	0.85		0.26	0.15	0.94	
	550		0.75	0.86		0.25	0.14	0.93	
	560		0.77	0.87		0.23	0.13	1.04	
	570		0.73	0.85		0.27	0.15	1.03	
	580		0.63	0.77		0.37	0.23	1.00	
	590		0.53	0.69		0.47	0.31	1.18	
dbr123	530	1.9	0.44	0.78	0.41	0.56	0.22	0.94	1.01
	540		0.54	0.84		0.46	0.16	0.99	
	550		0.58	0.86		0.42	0.14	1.03	
	560		0.64	0.89		0.36	0.11	0.94	
	570		0.65	0.89		0.35	0.11	0.95	
	580		0.52	0.83		0.48	0.17	0.99	
	590		0.39	0.74		0.61	0.26	1.09	
	600		0.27	0.62		0.73	0.38	1.19	

across all decay data and preexponential factors are allowed to float independently. Table II shows the results of such an analysis for **rh123** and **dbr123** in K562 cell lines. Individual χ^2 values for each decay data and global χ^2 values show that the analysis considering the two species model is reasonable. From the normalized preexponential factors, we have calculated the fractional contribution to the fluorescence intensity of each species. By multiplying this fraction with the steady-state fluorescence intensity at the corresponding wavelength, the emission spectrum associated to each species can be recovered. Such decay-associated spectra (DAS) corresponding to each species for **rh123** and **dbr123** in K562 cell lines together with the steady-state emission spectrum are shown in Fig. 5. Cell autofluorescence (without dye) is also shown in this figure (the background spectrum). This fluorescence background is found to be negligible compared to the steady-state fluorescence as well as DAS spectra in the wavelength region we have studied. From our earlier study,[24] we observed two intrinsic fluorescence bands, one in the 300- to 400-nm region and another in the 400- to 500-nm region, for these cell lines. Tryptophan and NADH residues are found to be responsible, respectively, for the shorter-wavelength fluorescence band (λ_{max} = 340 nm) and the longer-wavelength fluorescence band (λ_{max} = 450 nm). The above observations indicate that the two DAS spectra are coming from dye bound at two different binding sites.

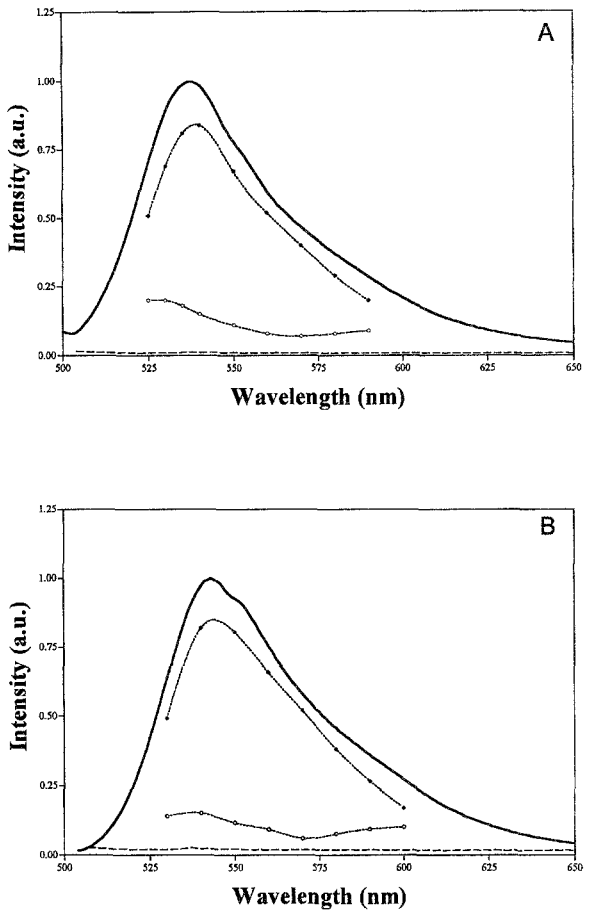

Fig. 5. Steady-state emission spectrum together with decay-associated spectra (DAS) of **rh123** (A) and **dbr123** (B) in K562 cell lines. (——) Steady-state spectrum. (-------) Longest-lifetime DAS. (---o---) Shortest-lifetime DAS. (—·—) Fluorescence background of the cell without the dye. The steady-state fluorescence spectrum of the dye and the background spectrum are taken at the same sensitivity. For DAS, symbols are the data obtained from the emission wavelength-dependent global analysis and the line is the cubic spline fit of the data.

From Table I, one can see that the lifetime of species **1** is similar to those obtained in SDS and in aqueous medium. Actually, for rhodamine dyes the lifetime is not a sensitive parameter concerning the binding with SDS micelles. Though the changes are within the limit of experimental error (± 10 %), for **dbr123** the lifetime (1.9 ns) of species **1** is slightly but consistently higher than that (1.7 ns) obtained for the free form (i.e., in aqueous/DPBS medium) and little less than the value (2.1 ns) obtained in SDS. On the other hand, DAS of species **1** is red shifted compared to its free form in an aqueous medium. Red shifting of the emission spectrum is also observed when rhodamine dyes are bound to SDS micelles. From these observations, one can conclude that

Table III. Global Analysis of the Fluorescence Decay of rh123 in K562 Cell Lines at Different Incubation Dye Concentration (Excitation Wavelength = 480 nm and Emission Wavelength Monitored at 540 nm)

[rh123] (μM)	τ_1 (ns)	α_1	I_1	τ_2 (ns)	α_2	I_2	Individual χ^2	Global χ^2
1	4.0	0.70	0.83	2.0	0.30	0.18	0.96	0.95
5		0.67	0.80		0.33	0.20	0.94	
10		0.71	0.83		0.29	0.17	0.98	
15		0.69	0.82		0.31	0.18	0.94	
20		0.685	0.81		0.32	0.19	0.93	

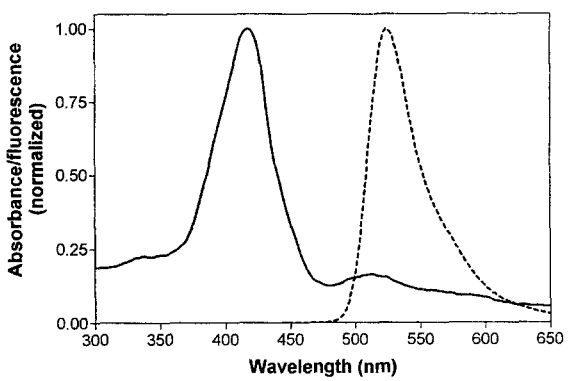

Fig. 6. Normalized absorption spectrum (——) of dilute suspension of extracted (K562 cell lines) mitochondria in DPBS and normalized emission spectrum (– – –) of **rh123** in DPBS.

species **1** is localized in more hydrophobic binding sites and is protected from the aqueous environment. The probable site of localization for species **1** is the negatively charged region of lipids in the mitochondria or any negatively charged protein embedded or in close proximity to the mitochondrial membrane.

In the case of species **2**, the fluorescence lifetime of the dye is decreased due to the quenching of fluorescence intensity. The DAS of species **2** is nearly identical to the fluorescence maximum of the free form of the dye in aqueous medium, while the DAS of species **1** is red shifted. The maximum for DAS of species **2** is not well resolved, particularly in the case of **rh123**, because we could not measure the fluorescence decay at shorter wavelengths due to the scattering coming from the excitation wavelength (480 nm). Fluorescence quenching of the probing dye in micellar and in biological membranes is not uncommon.[14,25–27] For rhodamine dyes, fluorescence quenching may arise for several reasons: due to aggregate formation, as aggregates of rhodamine dyes are nonfluorescent; due to charge-transfer complex formation, as is observed in the case of TX micelles, where the fluorescence lifetime of the rhodamine dye is decreased by the charge-transfer complex formation between rhodamine and the phenol moiety of TX; and due to resonance energy transfer (Förster type) between species **2** as a donor and some other component in the mitochondrial membrane as acceptor.

To check whether the decrease in lifetime is due to aggregate formation, we have studied the dye concentration (during incubation) dependence on lifetime parameters. A series of decay data is measured for different dye incubation concentrations and analyzed globally by linking lifetimes across all decay data and preexponential factors are allowed to float independently. Table III shows the results of such an analysis for **rh123**. χ^2 values in Table III are reasonable and hence support the two-species model for all **rh123** concentrations. Whether species **2** originates from aggregate formation, the preexponential factor corresponding to the shorter lifetime would increase with an increasing amount of dye inside the cell. Table III shows that preexponential factors obtained from global analysis for the two lifetimes are independent of the amount of dye present inside the cell. This result strongly suggests that the origin of species **2** is not due to aggregate formation. Also, as with time the living cells generally extrude all the dye bound to the mitochondria, if we keep the dye-bound cell in dye-free DPBS medium, the possibility of formation of a strong ground-state charge-transfer complex (due to which the fluorescence lifetime can be reduced) inside mitochondria is less realistic.

Resonance Energy Transfer

Förster-type resonance energy transfer (FRET) between a donor dye and an acceptor component in mitochondria of living cell is not uncommon. Recently Hüglin *et al.*[25] reported resonance energy transfer between pyrene derivative acting as donor and cytochrome *c* in the mitochondria of HeLa cell acting as an acceptor. The observation of a decrease in the fluorescence lifetime of pyrene was interpreted accordingly. The strong absorption band of the mitochondria (Fig. 6) is caused mainly by the cytochromes of the inner membrane system. The absorption spectrum of cytochrome is due to the porphyrin moiety present in the cytochrome and is characterized by the intense Soret band of porphyrins in the range 405–430 nm and weak flavine and ferredoxin bands in the 500- to 650-nm region. The energy transfer efficiency depends on the overlap between the donor fluorescence and the acceptor absorption bands. The distance between the two components involved in the

energy transfer should also be close enough. The pyrene fluorescence (in the range of 360–480 nm) has a strong overlap with the Soret band and hence energy transfer is favored. The rhodamine fluorescence (in the range of 500–650 nm) overlaps weakly with the flavine and ferredoxin band (see Fig. 6) because of the low extinction coefficient of the potential acceptor. Thus, the energy transfer between rhodamine and porphyrin in cytochrome seems less probable. To check whether this type of energy transfer might be effective, we have measured the fluorescence lifetime of **rh123** in the presence of the hydrophobic porphyrin derivative (POR10) in SDS micelles. This cationic porphyrin derivative with long hydrophobic chains was chosen for its solubility in SDS micelles. In fact, both dyes (porphyrin and rhodamine) solubilize in SDS micelles and the distance between them is less than 30 Å (average diameter of the SDS micelle[13]), but no quenching of **rh123** fluorescence is observed even at a high concentration of the porphyrin ([rh123] = 5×10^{-7} *M*, [porphyrin] = 2×10^{-5} *M*). This observation suggests that no energy transfer is feasible between rhodamine and the porphyrin moiety present in cytochrome *c*.

Another possible explanation for the decrease in the fluorescence lifetime of species **2** is the energy transfer from species **2** to species **1**. Small or negligible shifting of the DAS of species **2** compared to the emission in aqueous environment indicates that species **2** is bound to a less hydrophobic binding site and is close to the aqueous interface. So the steady-state emission spectrum of species **2** alone should be similar to that obtained for the free dye in an aqueous environment. As the contribution to the total emission of the dye bound to mitochondria is governed mainly by species **1** (see the I_1 and I_2 values in Tables II and III and Fig. 5), the excitation spectrum of species **1** should be similar to that obtained for the dye bound to mitochondria. From Fig. 2, one can see the strong overlap between the excitation spectrum of the bound dye and the emission spectrum of the free dye. This situation is in favor of an energy transfer taking place between species **2** and species **1**. Calculation of the overlap between excitation and fluorescence spectra of the donor and acceptor, respectively (see Fig. 2), shows that energy transfer is fivefold more probable from species **2** to species **1** than from species **1** to species **2**. In fact self-quenching of the fluorescence of rhodamine derivatives is not uncommon due to the small Stokes shift observed in these dyes. The observations of striking enhancements of self-quenching of lipid conjugated rhodamine in the liposomal[26,27] and bilayer lipid[28] membrane are explained in terms of Förster resonance energy transfer.

If τ and τ^0 are the fluorescence lifetime of the donor (species **2**) in the presence and absence of the acceptor (species **1**), respectively, according to the theory of Förster,[29–31] the efficiency E of the intermolecular energy transfer is given by

$$E = 1 - \tau/\tau^0 \tag{3}$$

It is important to note that this expression is applicable only to donor–acceptor pairs which are separated by a fixed distance R. In this condition, the fluorescence decay of the donor should be single exponential.[31] In fact, our fluorescence decay analysis shows that a single lifetime for each species is sufficient to explain the decay kinetics. A similar result was obtained recently on mitochondria of HeLa cells.[25] Indeed we have tried to fit other decay functions to our experimental results without any success. For nonexponential decays, several models can be considered:[32] FRET with a similar distribution of acceptors, FRET with an additional donor exponential decaying term when some donors are not affected by any acceptors, and finally, a function which takes into account the inhomogeneous broadening leading to a distribution of decay rates. In all cases the best fit to our data involved the function with only two exponential decays. Assuming this situation to be the real one, we can consider τ as the lifetime of species **2** after quenching has occurred and τ^0 as the lifetime obtained in a free aqueous environment. E is also related to R, the distance between the donor and the acceptor molecule as

$$R = (1/E - 1)^{1/6} R_0 \tag{4}$$

where R_0 is the Förster radius, which describe the donor–acceptor distance at 50% energy transfer. R_0 values for energy transfer to similar monomer rhodamine dyes in lipid membrane are reported in the literature.[26,33,34] Values are ranging between 51 and 58 Å, depending on the nature of the dye and membrane. Considering a reasonable R_0 value as 55 Å for both **rh123** and **dbr123**, we have calculated E and R values for both dyes in different cell lines and in extracted mitochondria. Values are tabulated in Table IV. This is a rough estimation in view of the model used, but the order of magnitude might be correct. For both dyes, values of R, i.e., the distance between species **1** and species **2**, are almost constant and are in the range of 46–56 Å. Lipid bilayers in biological membranes have thicknesses between 50 and 60 Å and a mitochondrial membrane consists of two membranes of lipid bilayers. The mean diameter of membrane proteins of the respiratory chain is of the same order of magnitude.[35] Our estimation of the distance between the two species is also of the same order. This indicates that the long-lived species, which is localized in a more hy-

Table IV. Data of Förster-Type Energy Transfer Efficiency (E) and the Distance (R) Between Acceptor Species (1) and Donor Species (2) of rh123 and dbr123 in Different Cell Lines and Mitochondria [Values Calculated from Eqs. (4) and (5) Using Fluorescence Lifetime data]

Dye	Medium	τ_0 (ns)	τ (ns)	E	R (Å)
rh123	K562 cell	4.2	2.0	0.52	54
	KG1 cell	4.2	2.1	0.51	55
	Rat 2 cell	4.2	2.2	0.48	56
	Mitochondria (K562)	4.2	2.0	0.52	54
	Mitochondria (KG1)	4.2	2.0	0.53	54
dbr123	K562 cell	1.7	0.41	0.75	46
	KG1 cell	1.7	0.5	0.70	48
	Rat 2 cell	1.7	0.56	0.66	49
	Mitochondria (K562)	1.7	0.57	0.65	50
	Mitochondria (KG1)	1.7	0.54	0.67	49

drophobic region, may be bound with some hydrophobic membrane protein and the short-lived species is localized in a less hydrophobic region, at the aqueous interface with the bilayer lipid. The possibility of the binding of the cationic dye with mitochondrial proteins has been reported in the literature.[36,37] Our results also support this kind of interaction.

CONCLUDING REMARKS

Steady-state spectroscopic properties together with fluorescence microscopy in different cell lines and in extracted mitochondria reveal that these dyes specifically bind with mitochondria. Excitation and emission spectra of the bound dyes are red shifted by 10–12 nm compared to the free form. The nature of localization of the dye in the mitochondria of the cell lines is found to be independent of whether cell lines are highly tumorigenic or normal.

The observation of two lifetimes indicates that these dyes bind to the mitochondria at two different binding sites. Global analysis of emission wavelength and dye concentration dependence of fluorescence decay reveals that the binding site corresponding to the longer lifetime is more hydrophobic than that corresponding to the shorter lifetime.

The fluorescence of the shorter-lifetime species might be explained using a quenching mechanism. The Förster type of resonance energy transfer between the shorter-lifetime species (donor) and the longer-lifetime species (acceptor) is found to be a reasonable explanation for this fluorescence quenching. From fluorescence lifetimes, the efficiency of energy transfer (E) and the distance (R) between the two species are evaluated. For both dyes, R values are found to be reasonable relative to the dimension of lipid bilayers of the biological membranes.

ACKNOWLEDGMENTS

This work was supported by a grant from Theratechnologies Inc., Montreal, Canada. One of us (G.D.) would like to thank the Natural Sciences and Engineering Research Council of Canada and the "Fonds FCAR" (Québec) for financial assistance in the form of grants.

REFERENCES

1. L. V. Johnson, M. L. Walsh, and L. B. Chen (1980) *Proc. Natl. Acad. Sci. USA* **77**, 990.
2. C. R. Shea, M. E. Sherwood, T. J. Flotte, N. Chen, M. Scholz, and T. Hasan (1990) *Cancer Res.* **50**, 4167.
3. L. B. Chen (1989) *Methods Cell Biol.* **29**, 103.
4. G. Iron, L. Ochsenfeld, A. Naujok, and H. W. Zimmermann (1993) *Histochemistry* **99**, 75.
5. L. V. Johnson, M. L. Walsh, B. J. Bockus, and L. B. Chen (1981) *J. Cell Biol.* **88**, 526.
6. P. Morliere, P. Santus, M. Bazin, E. Kohen, V. Carillet, F. Bon, J. Rainasse, and L. Dubertret (1992) *Photochem. Photobiol.* **52**, 703.
7. P. Pal, H. Zeng, G. Durocher, D. Girard, T. Li, A. K. Gupta, R. Giasson, L. Blanchard, L. Gaboury, A. Balassy, C. Turmel, A. Laperrière, and L. Villeneuve (1996) *Photochem. Photobiol.* **63**, 161.
8. J. L. Weaver, P. S. Pine, A. Asxalos, P. V. Schoenlein, S. J. Currier, R. Padmanabhan, and M. M. Gottesmann (1991) *Exp. Cell Res.* **196**, 323.
9. K. Kalyanasundaram (1991) in V. Ramamurthy (Ed.), *Photochemistry in Organized and Constrained Media*, VCH, New York.
10. J. R. Lakowicz, P. A. Koen, H. Szmacinski, I. Gryczysski, and J. Kusba (1994) *J. Fluoresc.* **4(1)**, 117.
11. J. M. Beechem (1989) *Chem. and Phys. Lipids* **50**, 237.
12. L. D. Janssents, N. Boens, M. Ameloot, and F. C. De Schryver (1990) *J. Phys. Chem.* **94**, 3564.
13. J. H. Fendler (1982) in *Membrane Mimetic Chemistry*, Wiley Interscience, New York.
14. P. Pal, H. Zeng, G. Durocher, D. Girard, R. Giasson, L. Blanchard, L. Gaboury, and L. Villeneuve (1996) *J. Photochem. Photobiol. A Chem.* (in press).
15. Y. Okuno, W. E. Ford, and M. Kelvin (1980) *Synthesis* 537–539.
16. R. S. Sarpal, M. Belletête, and G. Durocher (1993) *J. Phys. Chem.* **97**, 5007.
17. A. Chow, J. Kennedy, R. Pottier, and T. G. Truscott (1986) *Photobiochem. Photobiophys.* **11**, 139.
18. C. Demonacos, R. Djordjevic-Markovic, N. Tsawdaroglou, and C. E. Sekeris (1993) *J. Steroid Biochem. Mol. Biol.* **46**, 401. E. A. Siess (1983) *Physiol. Chem.* **364**, 279.
19. B. Zelent, T. Ganguly, L. Farmer, D. Gravel, and G. Durocher (1991) *J. Photochem. Photobiol. A* **56**, 165.
20. *Global Unlimited*, Version 1.02-2 (1990), updated in 1993 (Laboratory for Fluorescence Dynamics, University of Illinois at Urbana–Champaingn).
21. N. Shinomiya, S. Tsuru, Y. Katsura, I. Sekiguchi, M. Suzuki, and K. Nomoto (1992) *Exp. Cell Res.* **198**, 159.

22. J. S. Lee, K. Paull, M. Alvarez, C. Hose, A. Monks, M. Grever, A. T. Fojo, and S. E. Bates (1994) *Mol. Pharmacol.* **46**, 627.
23. J. M. Millot, S. Sharonov, and M. Manfait (1994) *Cytometry* **17**, 50.
24. A. Pradhan, P. Pal, G. Durocher, L. Villeneuve, A. Balassy, F. Babai, L. Gaboury, and L. Blanchard (1995) *J. Photochem. Photobiol. B Biol.* **31**, 101.
25. D. Hüglin, W. Seiffert, and H. W. Zimmermann (1995) *J. Photochem. Photobiol. B Biol.* **31**, 145.
26. R. I. MacDonald (1990) *J. Biol. Chem.* **265**, 13533.
27. B. Aroeti and Y. I. Henis (1987) *Exp. Cell Res.* **179**, 322.
28. J. Karolin, S. T. Boben, L. B. Å. Johansson, and J. G. Molotkovsky (1995) *J. Fluoresc.* **5**, 279.
29. Th. Förster (1951) in *Fluoreszenz organischer Verbindungen*, Vandenhoeck und Ruprecht, Göttingen.
30. I. Z. Steinberg, E. Haas, and E. Katchalski-Katzir (1983) in, R. B. Cundall and R. E. Dale (Eds.), *Time-Resolved Fluorescence Spectroscopy in Biochemistry and Biology*, (ed.) Plenum, New York, p. 441.
31. J. R. Lakowicz (1983) in *Principles of Fluorescence Spectroscopy*, Plenum, New York, p. 306.
32. P. Ballet, M. Van Der Auweraer, F. C. De Schryver, H. Lemmetyinen, and E. Vuorimaa (1996) *J. Phys. Chem.* **100**, 13701.
33. R. F. Chen and J. R. Knutson (1988) *Anal. Biochem.* **172**, 61.
34. K. K. Rohatgi and G. S. Singal (1972) *J. Phys. Chem.* **69**, 1894.
35. C. R. Hackenbrock, S. S. Gupta, and B. Chazotte (1985) in E. Quagliariello, E. C. Slater, F. Palmieri, C. Saccone, and A. M. Kroon (Eds.), *Achievements and Perspectives of Mitochondrial Research, Vol. I. Bioenergetics*, Elsevier, Amsterdam. pp. 83.
36. K. Schneider and H. W. Zimmermann (1994) *Histochemistry* **101**, 135.
37. K. Schneider, A. Naujok, and H. W. Zimmermann (1994) *Histochemistry* **101**, 455.